

## Seasonal Dependence in the Solar Neutrino Flux

P. C. de Holanda<sup>1,2</sup>, C. Peña-Garay<sup>1</sup>, M. C. Gonzalez-Garcia<sup>1</sup>, and J. W. F. Valle<sup>1</sup>

<sup>1</sup> *Instituto de Física Corpuscular – C.S.I.C.*

*Departamento de Física Teòrica, Universitat of València*

*46100 Burjassot, València, Spain*

*http://neutrinos.uv.es*

<sup>2</sup> *Instituto de Física Gleb Wataghin*

*Universidade Estadual de Campinas, UNICAMP 13083-970 – Campinas, Brazil*

MSW solutions of the solar neutrino problem predict a seasonal dependence of the zenith angle distribution of the event rates, due to the non-zero latitude at the Super-Kamiokande site. We calculate this seasonal dependence and compare it with the expectations in the no-oscillation case as well as just-so scenario, in the light of the latest Super-Kamiokande 708-day data. The seasonal dependence can be sizeable in the large mixing angle MSW solution and would be correlated with the day-night effect. This may be used to discriminate between MSW and just-so scenarios and should be taken into account in refined fits of the data.

The difference in the  $\nu_e$  fluxes during the day and the night due to the regeneration of the  $\nu_e$  in the earth matter – the so-called day-night effect – is one of the milestones of the MSW solutions of the solar neutrino problem (SNP) [1,2]. This effect is negligible in the just-so picture [3]. Conversely, it is well-known that vacuum oscillations lead to a seasonal effect due to the fact that the distance between the Earth and the Sun changes in different seasons of the year leading to different predicted event rates beyond the simple geometrical factor. Though recognized in the early days of the MSW effect [4] the seasonal effect has been neglected in most discussions of the MSW solution to the SNP and has even been recently claimed to be absent in the MSW picture [5,6].

Recent Super-Kamiokande data after 708 days [7] exhibit an excess of the number of events during the night [8]. Though not yet statistically significant this provides some hint in favor of the possible existence of a day-night effect. On the other hand there is also some hint for a seasonal variation in these data, especially for recoil electron energy above 11.5 MeV. While the former would be an indication in favour of the MSW solution, the latter would favour the just-so solution.

Here we call the attention to this interesting feature of the MSW solution, namely that the expected MSW event rates do exhibit a seasonal effect due to the different night duration throughout the year at the experimental site, which leads to a seasonal-dependent  $\nu_e$  regeneration effect in the Earth. Taking into account the relative position of the Super-Kamiokande setup in each period of

the year, we calculate the distribution of the events along the year both for the large mixing angle (LMA) and the small mixing angle (SMA) solutions to the SNP. We find that the effect can be as large as the one expected in the just-so scenario, especially in the LMA solution, where it amounts to  $\sim 10\%$  at the best fit point for the solar neutrino event rates given by [9]. For the SMA solution we find that the magnitude of the seasonal MSW effect is very small at the best fit point increasing as  $\sin^2 2\theta$  increases within the 99% CL region. We illustrate this behaviour in Figs. 1 and 2 and in table I.

Let us now describe our calculation. For simplicity, let us consider the two-neutrino mixing case

$$\nu_e = \cos\theta \nu_1 + \sin\theta \nu_2, \quad \nu_\mu = -\sin\theta \nu_1 + \cos\theta \nu_2, \quad (1)$$

We have determined the solar neutrino survival probability  $P_{ee}$  in the usual way, assuming that the neutrino state arriving at the Earth is an incoherent mixture of the  $\nu_1$  and  $\nu_2$  mass eigenstates.

$$P_{ee} = P_{e1}^{Sun} P_{1e}^{Earth} + P_{e2}^{Sun} P_{2e}^{Earth} \quad (2)$$

where  $P_{e1}^{Sun}$  is the probability that a solar neutrino, that is created as  $\nu_e$ , leaves the Sun as a mass eigenstate  $\nu_1$ , and  $P_{1e}^{Earth}$  is the probability that a neutrino which enters the Earth as  $\nu_1$  arrives at the detector as  $\nu_e$ . Similar definitions apply to  $P_{e2}^{Sun}$  and  $P_{2e}^{Earth}$ .

The quantity  $P_{e1}^{Sun}$  is given, after discarding the oscillation terms, as

$$P_{e1}^{Sun} = 1 - P_{e2}^{Sun} = \frac{1}{2} + \left(\frac{1}{2} - P_{LZ}\right) \cos[2\theta_m(r_0)] \quad (3)$$

where  $P_{LZ}$  denotes the standard Landau-Zener probability [10] and  $\theta_m(r_0)$  is the mixing angle in matter at the neutrino production point. In our calculations of the expected event rates we have averaged this probability with respect to the production point assuming the production point distribution given in [11].

In order to obtain  $P_{ie}^{Earth}$  we integrate the evolution equation in matter assuming a step-function profile of the Earth matter density. In the notation of Ref. [12], we obtain for  $P_{2e}^{Earth} = 1 - P_{1e}^{Earth}$

$$P_{2e}^{Earth}(\Phi) = (Z \sin \theta)^2 + (W_1 \cos \theta + W_3 \sin \theta)^2 \quad (4)$$

where  $\theta$  is the mixing angle in vacuum and the Earth matter effect is included in the formulas for  $Z, W_1$  and  $W_3$ , which can be found in Ref. [12].  $P_{2e}^{Earth}$  depends on the amount of Earth matter travelled by the neutrino in its way to the detector, or, in other words, on its arrival direction which is usually parametrized in terms of the nadir angle,  $\Phi$ , of the sun at the detector site.

It is very important to realize that the daily range of variation of the nadir angle depends on the period of the year. As a result the quantity  $P_{2e}^{Earth}$  is seasonal dependent. This will, in turn, manifest itself as a seasonal dependence of the expected neutrino event rates. The general expression of the expected signal in the presence of oscillations at a given time  $t$ ,  $S^{osc}(t)$ , is

$$S^{osc}(t) = \int dE_\nu \lambda(E_\nu) \times [\sigma_e(E_\nu) P_{ee}(E_\nu, t) + \sigma_x(E_\nu)(1 - P_{ee}(E_\nu, t))], \quad (5)$$

where  $E_\nu$  is the neutrino energy,  $\lambda$  is the neutrino energy spectrum [13] with the latest normalization [14],  $\sigma_e$  ( $\sigma_x$ ) is the  $\nu_e$  ( $\nu_x$ ,  $x = \mu, \tau$ ) interaction cross section in the Standard Model [15], and  $P_{ee}$  is the  $\nu_e$  survival probability, which varies in time through the interval of day and night along the year. The expected signal in the absence of oscillations,  $S^{no-osc}$ , can be obtained from Eq.(5) by substituting  $P_{ee} = 1$ .

The cross sections  $\sigma_{e,x}$  are calculated including radiative corrections and must be corrected for energy threshold and resolution effects. In the calculation of the expected signal it is understood that the  $\nu_\alpha$ - $e$  cross sections  $\sigma_\alpha(E)$  ( $\alpha = e, x$ ) have to be properly corrected to take into account the detector energy resolution and the analysis window for each experiment. In Super-Kamiokande, the finite energy resolution implies that the *measured* kinetic energy  $T$  of the scattered electron is distributed around the *true* kinetic energy  $T'$  according to a resolution function  $Res(T, T')$  of the form [16]:

$$Res(T, T') = \frac{1}{\sqrt{2\pi}s} \exp \left[ -\frac{(T - T')^2}{2s^2} \right], \quad (6)$$

where

$$s = s_0 \sqrt{T'/\text{MeV}}, \quad (7)$$

and  $s_0 = 0.47$  MeV for Super-Kamiokande [7,17]. On the other hand, the distribution of the true kinetic energy  $T'$  for an interacting neutrino of energy  $E_\nu$  is dictated by the differential cross section  $d\sigma_\alpha(E_\nu, T')/dT'$ , that we take from [15]. The kinematic limits are:

$$0 \leq T' \leq \bar{T}'(E_\nu), \quad \bar{T}'(E_\nu) = \frac{E_\nu}{1 + m_e/2E_\nu}. \quad (8)$$

For assigned values of  $s_0, T_{\min}$ , and  $T_{\max}$ , the corrected cross section  $\sigma_\alpha(E_\nu)$  is defined as:

$$\sigma_\alpha(E_\nu) = \int_{T_{\min}}^{T_{\max}} dT \int_0^{\bar{T}'(E_\nu)} dT' Res(T, T') \frac{d\sigma_\alpha(E_\nu, T')}{dT'}. \quad (9)$$

Finally, in order to compare our results with the recent data from Super-Kamiokande collaboration, we must also include the geometrical seasonal neutrino flux variation due to the variation of the Sun-Earth distance ( $L \approx 1.5 \times 10^{13}$  cm) arising from the Earth's orbit eccentricity because the neutrino fluxes in Eq.(5) are yearly averages. In order to account for this effect we assume a  $1/L^2$  dependence of the flux. Notice that Super-Kamiokande data are presented as ratio of observed events over the expected number in the Standard Solar Model where this expected number of events does not include the geometrical variation. Thus we must compare the experimental points with the predictions:

$$\frac{N_{osc}(t_0, \Delta t)}{N_{no-osc}(\Delta t)} = \frac{\int_{t_0 - \Delta t/2}^{t_0 + \Delta t/2} dt \frac{S^{osc}(t)}{\hat{L}^2(t)}}{\Delta t S^{no-osc}} \quad (10)$$

where

$$\hat{L}(t) = \left[ 1 - \epsilon \cos 2\pi \frac{t}{T} \right] \quad (11)$$

and  $\epsilon = 0.0167$  is the eccentricity of the Earth's orbit around the Sun, and  $T = 1$  year.

We now turn to our results. In order to study the behaviour of the seasonal variation we have explored the parameter space around the small and large mixing angle solutions, SMA and LMA, respectively. We find that depending on the values of the mass and mixing angle, one may get either an enhancement or a damping of the geometrical effect or even more complicated variations of the signals.

In Fig. 1 we present the expected event numbers in the recoil electron energy range from 11.5 MeV up to the maximum, plotted versus the period of the year for different points in the SMA solution region of the SNP divided by the BP98 SSM predictions in the absence of neutrino conversions [14]. We plot the expected behaviour for three points: the best fit point obtained by [9] with an arbitrary  ${}^8B$  flux,  $\Delta m^2 = 5. \times 10^{-6}$  eV<sup>2</sup>

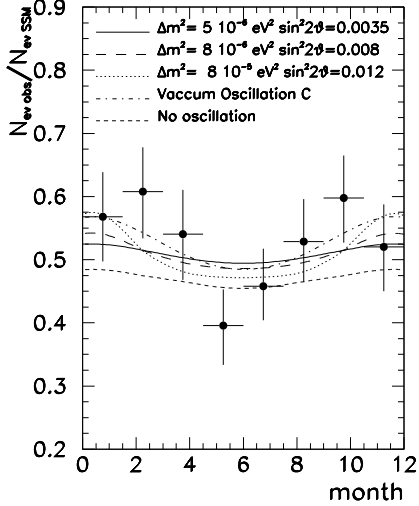


FIG. 1. Ratio of predicted event rate to the SSM prediction versus time of the year in Super-Kamiokande for various points in the SMA solution region of the SNP as labelled. We have normalized these three curves to the same yearly averaged event rate which corresponds to  ${}^8B$  flux normalization 0.7 for the best fit point. We also show the expectation in the absence of oscillations with  ${}^8B$  flux normalization of 0.47 (short dashed line) and the expected effect in case of vacuum oscillations for solution C in Ref. [6] (dash-dotted curve). The 708 Super-Kamiokande data points are also displayed.

and  $\sin^2 2\theta = 3.5 \times 10^{-3}$ , a point inside the 99% confidence level allowed region with  $\Delta m^2 = 8. \times 10^{-6} \text{ eV}^2$  and  $\sin^2 2\theta = 8. \times 10^{-3}$  and a near point with  $\Delta m^2 = 8. \times 10^{-6} \text{ eV}^2$  and  $\sin^2 2\theta = 1.2 \times 10^{-2}$ . We have normalized these three curves to the same yearly averaged event rate. This corresponds to a  ${}^8B$  flux normalization 0.7 for the best fit point. For the sake of comparison we also plot the expected behaviour in the absence of oscillations with  ${}^8B$  flux normalization of 0.47 as well as the best fit point for the vacuum solution C of Ref. [6].

As seen in the figure the seasonal effect is comparable to the expectation in the absence of oscillation at the best fit point of the SMA solution and it increases as the mixing angle increases. In Table I we show the seasonal variation (in percent) defined as

$$Var \equiv 2 \frac{R_{max} - R_{min}}{R_{max} + R_{min}}$$

for the different MSW and vacuum solutions of the SNP where  $R(t) = N_{osc}(t)/N_{SSM}$ . We find that for the SMA solution the effect increases as one increases  $\sin^2 2\theta$ . For example for  $\sin^2 2\theta = 0.008$ , still within the 99 % CL allowed region, it reaches 10% and for  $\sin^2 2\theta = 0.012$  it gets to be as large as 20%. Of course, since the seasonal effect is induced by the variation of the regeneration in the Earth along the year, the effect is large only in the parameter region where the day-night effect is not neg-

Point	$\Delta m^2 \text{ (eV}^2\text{)}$	$\sin^2(2\theta)$	Var (%)
No-oscillation			6
MSW SMA			
Best Fit Point	$5 \times 10^{-6}$	$3.5 \times 10^{-3}$	6
	$8 \times 10^{-6}$	$8 \times 10^{-3}$	10
	$8 \times 10^{-6}$	$1.2 \times 10^{-2}$	20
MSW LMA			
Best Fit Point	$1.6 \times 10^{-5}$	0.57	10
	$1. \times 10^{-5}$	0.6	22
	$3.2 \times 10^{-5}$	0.6	9
Vacuum Solutions			
C	$4.4 \times 10^{-10}$	0.93	15
D	$6.4 \times 10^{-10}$	1	12
A	$6.5 \times 10^{-11}$	0.7	9

TABLE I. Seasonal variation (in percent) of the ratio of predicted event rate in various oscillation scenarios to the SSM prediction.

ligible, which corresponds to larger mixing angle values. Note that in the SMA region the points we have chosen in order to illustrate the possible seasonal variation in the MSW picture are consistent with the measured yearly average day-night asymmetry.

Now we turn to the LMA solution of the SNP where the effects are potentially larger. Our results for this case are displayed in Fig. 2. Again, we plot the expected behaviour for three characteristic points: the best fit point obtained by [9] with an arbitrary  ${}^8B$  flux ( $\sin^2 2\theta = 0.57$ ,  $\Delta m^2 = 1.6 \times 10^{-5} \text{ eV}^2$ ), a point inside the 99% confidence level allowed region with  $\Delta m^2 = 1. \times 10^{-5} \text{ eV}^2$  and  $\sin^2 2\theta = 0.6$  and a point inside the allowed region where the expected average day-night asymmetry is smaller,  $\Delta m^2 = 3.2 \times 10^{-5} \text{ eV}^2$  and  $\sin^2 2\theta = 0.6$ . We have normalized these three curves to the same yearly averaged event rate. This corresponds to a  ${}^8B$  flux normalization 1.45 for the best fit point. We also plot the expected behaviour in the absence of oscillations with  ${}^8B$  flux normalization of 0.47 and the best fit vacuum solution C from Ref. [6]. In Table I we show the variation (in percent) corresponding to these points. As seen in the table the effect at the best fit point of the LMA solution (10 %) is comparable with the corresponding effect in some of the favoured vacuum oscillation solutions. In the LMA solution region the seasonal variation is very mildly dependent on the mixing angle while presents an oscillatory variation with  $\Delta m^2$ . Our results show that depending on the mass and mixing angle values one may get an enhancement or damping of the geometrical effect. We must bear in mind, however, than in the lower  $\Delta m^2$  part of the LMA solution region, the expected yearly average day-night asymmetry is in conflict with the existing data.

Finally let us comment on the effect of an enhanced hep neutrino flux as suggested in [18] in order to ac-

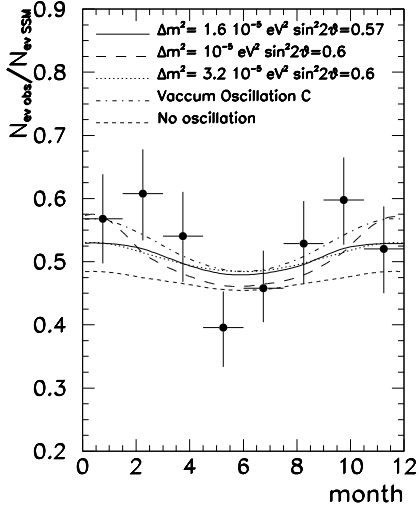


FIG. 2. Ratio of predicted event rate to the SSM prediction versus time of the year in Super-Kamiokande for various LMA solutions of the SNP labelled in the figure. These three curves are normalized to the same yearly averaged event rate corresponding to a  ${}^8\text{B}$  flux normalization 1.45 for the best fit point. We also show the expectation in the absence of oscillations with  ${}^8\text{B}$  flux normalization of 0.47 (short dashed line) and the expected effect for vacuum oscillation solution C in Ref. [6] (dash-dotted curve) together with the 708 Super-Kamiokande data points.

count for the recent Super-Kamiokande measurements of the energy spectrum. We find that even with large hep enhancement factors of 20 or more, the expected modifications of our results near the best fit points both for the SMA and LMA are small.

To summarize, we have shown that MSW solutions of the solar neutrino problem can lead to a sizeable seasonal dependence of the event rates in the large mixing angle region and this should be taken into account in refined fits of the data where the day-night analysis is also performed. The MSW seasonal effect is correlated with the day-night asymmetry and may potentially be useful in order to pinpoint the underlying mechanism involved in the explanation of the solar neutrino anomaly, discriminating between different solutions. For example, the non-observation of the day-night effect and the confirmation of seasonal-dependent rates would provide an indication for the just-so picture. Conversely, a possible confirmation of a seasonal dependence accompanied by the day-night effect would point towards a LMA MSW-type solution.

We are grateful to E. Akhmedov and C. Yanagisawa for useful comments. This work was supported by Spanish DGICYT under grant PB95-1077, by the European Union TMR network ERBFMRXCT960090. P. C. de Holanda was supported by FAPESP (Brazil).

- 
- [1] S. P. Mikheyev and A. Yu. Smirnov, '86 *Massive Neutrinos in Astrophysics and in Particle Physics*, proceedings of the Sixth Moriond Workshop, edited by O. Fackler and J. Trân Thanh Vân (Editions Frontières, Gif-sur-Yvette, 1986), pp. 355
  - [2] J. Bouchez *et al.*, *Z. Phys.* **C32**, 499 (1986); E. D. Carlson, *Phys. Rev.* **D34**, 1454 (1986) ; A.J. Baltz and J. Weneser, *Phys. Rev.* **D50**, 5971 (1994); A. J. Baltz and J. Weneser, *Phys. Rev.* **D51**, 3960 (1995); P. I. Krastev, hep-ph/9610339; Q.Y. Liu, M. Maris and S.T. Petcov, *Phys. Rev.* **D56**, 5991 (1997); J.N. Bahcall and P.I. Krastev, *Phys. Rev.* **C56**, 2839 (1997)
  - [3] S. L. Glashow and L.M. Krauss, *Phys. Lett.* **B19**, 199 (1987); A. Acker, S. Pakvasa and J. Pantaleone, *Phys. Rev. Lett.* **65**, 2479 (1990) and *Phys. Rev.* **D43**, 1754 (1991); V. Barger *et al.*, *Phys. Rev.* **D43**, 1110 (1991); V. Barger *et al.*, *Phys. Rev. Lett.* **69**, 3135 (1992); P.I. Krastev and S.T. Petcov, *Phys. Lett.* **B299**, 99 (1993) 99; S.L. Glashow, P.J. Kernan and L. Krauss, hep-ph/9808470
  - [4] A. J. Baltz and J. Weneser, *Phys. Rev.* **D35**, 528 (1987); A. J. Baltz and J. Weneser, *Phys. Rev.* **D37**, 3364 (1988);
  - [5] M. Maris, S. T. Petcov, SISSA 13/99/EP, hep-ph/9903303.
  - [6] V. Barger, K. Whisnant, hep-ph/9903262.
  - [7] Super-Kamiokande Collaboration, Y. Fukuda *et al.*, *Phys. Rev. Lett.* **82**, 1810 (1999).
  - [8] Y. Suzuki, talk given at *17th International Workshop on Weak Interactions and Neutrinos*, Cape Town, South Africa, January 1999; M.B. Smy, talk at *DPF-99*, Los Angeles, California, January 1999, hep-ex/9903034.
  - [9] J. N. Bahcall, P. I. Krastev and A. Yu. Smirnov, *Phys. Rev.* **D58**, 096016 (1998).
  - [10] P. I. Krastev, *Phys. Lett.* **B200**, 373 (1988); P. I. Krastev and S. T. Petcov, *Phys. Lett.* **B207**, 64 (1988)
  - [11] <http://www.sns.ias.edu/~jnb/SNdata/Export/Models/bp98flux.dat>; J. N. Bahcall, S. Basu and M. H. Pinsonneault, *Phys. Lett.* **B433**, 1, (1998).
  - [12] E.Kh.Akhmedov, *Nucl. Phys.* **B538**, 25 (1999).
  - [13] J. N. Bahcall, E. Lisi, D. E. Alburger, L. De Braeckeleer, S. J. Freedman, and J. Napolitano, *Phys. Rev.* **C54**, 411 (1996).
  - [14] J. N. Bahcall, S. Basu, and M.H. Pinsonneault, *Phys. Lett.* **B 433**, 1 (1998).
  - [15] J. N. Bahcall, M. Kamionkowsky, and A. Sirlin, *Phys. Rev.* **D51**, 6146 (1995).
  - [16] See, e.g. J. N. Bahcall, P. I. Krastev, and E. Lisi, *Phys. Rev.* **C55**, 494 (1997).
  - [17] B. Fäid, G. L. Fogli, E. Lisi and D. Montanino, *Astropart. Phys.* **10**, 93 (1999).
  - [18] J. N. Bahcall, P. I. Krastev, *Phys. Lett.* **B436**, 243 (1998); R. Escribano *et al.*, *Phys. Lett.* **B444**, 397 (1998).